References

About I. and Mitsiadis T.A. (2002). Molecular aspects of tooth pathogenesis and repair: in vivo and in vitro models. Adv. Dent. Res. 15, 59-62.

Acosta D., Puckett M. and McMillin R. (1978). Ischemic myocardial injury in cultured heart cells: leakage of cytoplasmic enzymes from injured cells. In Vitro. 14, 728-732.

Agata H., Kagami H., Watanabe N. and Ueda M. (2008). Effect of ischemic culture conditions on the survival and differentiation of porcine dental pulp-derived cells. Differentiation. 76, 981-993.

Amemiya K Kaneko Y. Muramatsu T, Shimono M, Inoue T. (2003). Pulp cell responses during hypoxia and reoxygenation in vitro. Eur. J. Oral Sci. 111, 332-338.

Aranha AM., Zhang Z., Neiva KG., Costa CA., Hebiling J. and Nor JE. (2010). Hypoxia enhances the angiogenic potential of human dental pulp cells. J Endod. 36, 1633-1637.

Bernert G., Hoeger H., Mosgoeller W., Stolzlechner D. and Lubec B. (2003). Neurodegeneration, neuronal loss, and neurotransmitter changes in the adult guinea pig with perinatal asphyxia. Pediatr. Res. 54, 523-528.

Das R, Jahr H, van Osch GJ, Farrell E. (2010). The role of hypoxia in bone marrow-derived mesenchymal stem cells: considerations for regenerative medicine approaches. Tissue Eng. Part B Rev. 16, 159-168.

Fukuyama Y, Ohta K, Okoshi R, Suehara M, Kizaki H, Nakagawa K. (2007). Hypoxia induces expression and activation of AMPK in rat dental pulp cells. J. Dent. Res. 86, 903-907.

Gronthos S., Mankani M., Brahim J., Gehron Robey P. and Shi S. (2000). Postnatal human dental pulp stem cells (DPSCs) in vitro and in vivo. Proc. Natl. Acad. Sci. USA. 97, 13625-13630

Gronthos S., Brahim J., Li W., Fisher L.W., Cherman N., Boyde A., Denbesten P., Robey P.G. and Shi S. (2002). Stem cell properties of human dental pulp stem cells. J. Dent. Res. 86, 531-535.

Iida K., Takeda-kawaguchi T., Tezuka Y., Kunisada T., Shibata T. and Tezuka K. (2010). Hypoxia enhances colony formation and proliferation but inhibits differentiation of human dental pulp cells. Arch Oral Biol. 55. 648-54.

Iohara K., Zheng L., Ito M., Tomokiyo A., Matsushita K. and Nakashima M. (2006). The side population cells isolated from porcine dental pulp tissue with self-renewal and multipotency for dentinogenesis, chondrogenesis, adipogenesis and neurogenesis. Stem Cells. 24, 2493-2503.

Jones S.M., Novak A.E. and Elliott JP. (2011). Primary culture of cellular subtypes from postnatal mouse for in vitro studies of oxygen glucose deprivation. J. Neurosci. Methods. 199, 241-248.

Li L., Zhu YQ., Jiang L., Peng W. and Ritchie HH. (2011). Hypoxia promotes mineralization of human dental pulp cells. J Endod. 37. 799-802.

Liu H., Gronthos S. and Shi S. (2006). Dental pulp stem cells. Methods. Enzymol. 419, 99-113.

Lennon DP, Edmison JM, Caplan AI. (2001). Cultivation of rat marrow-derived mesenchymal stem cells in reduced oxygen tension: effects on in vitro and in vivo osteochondrogenesis. J. Cell Physiol. 187, 345-355.

Rodrigues CA., Fernandes TG., Diogo MM., de Silva CL. and Cabral JM. (2010). Hypoxia enhances proliferation of mouse embryonic stem cell-derived neural stem cells. Biotechnol Bioeng. 106, 260-270.

Sakdee JB., White RR., Pagonis TC. and Hauschka PV. (2009). Hypoxia-amplified proliferation of human dental pulp cells. J Endod. 35, 818-823.

Sloan A.J. and Smith A.J. (2007). Stem cells and the dental pulp: potential roles in dentine regeneration and repair. Oral. Dis. 13, 151-157.

Sheridan A.M. and Bonventre J.V. (2000). Cell biology and molecular mechanisms of injury in ischemic acute renal failure. Curr. Opin. Nephrol. Hypertens. 9, 427-434.

Shinzawa K. and Tsujimoto Y. (2003) PLA_2 activity is required for nuclear shrinkage in caspase-independent cell death. J. Cell. Biol. 163, 1219-1230.

Spahr A., Lyngstadaas S.P., Slaby I., Haller B., Boeckh C., Tsoulfidou F. and Hammarström L. (2002). Expression of amelin and trauma-induced dentin formation. Clin. Oral. Investig. 6, 51-57.

Sugiyama M., Iohara K., Wakita H., Hattori H., Ueda M., Matsushita K. and Nakashima M. (2011). Dental pulp-derived $CD31^-/CD146^-$ side population stem/progenitor cells enhance recovery of focal cerebral ischemia in rats. Tissue. Eng. Part A. 17, 1303-1311.

Tsukamoto-Tanaka H, Ikegame M, Takagi R, Harada H, Ohshima H. (2006). Histochemical and immunocytochemical study of hard tissue formation in dental pulp during the healing process in rat molars after tooth replantation. Cell Tissue Res. 325, 219-229.

Ueno Y, Kitamura C, Terashita M, Nishihara T. (2006). Re-oxygenation improves hypoxia-induced pulp cell arrest. J. Dent. Res. 85, 824-828.

Wang J., Wei X., Ling J., Huang Y. and Gong Q. (2010). Side population increase after simulated transient ischemia in human dental pulp cell. J. Endod. 36, 453-458.

Figure legends

Figure 1

Changes in the expression of odontogenic/ osteogenic genes in non-induced and induced pDPCs cultured under severe-hypoxic conditions

Induced and non-induced pDPCs were cultured under severe hypoxic conditions in either low or high glucose concentration. Gene expression was analyzed by RT-PCR at 0, 6, 12 and 24 hours. Expression of Runx2, ALP, OP, TGFβ1, and α-SMA was slightly inhibited in both non-induced and induced cells. The expression of BSP, DMP-1, and DSPP was strongly inhibited in both populations. Non-induced and induced pDPCs underwent de-differentiation in a time-dependent manner. (From Agata *et al.*, 2008 with modification)

Figure 2

Viability of porcine dental pulp-derived cells (pDPCs) in cell culture depends on ischemic conditions

To investigate the effect of differential ischemic conditions, pDPCs were cultured under a range of O_2 concentrations (normoxia, hypoxia, or severe-hypoxia) and glucose concentrations (high glucose, low glucose, or glucose (-)) in serum-free media.

Viable cell number was calculated as the percentage of surviving cells. Significantly more cells survived under normoxic and hypoxic conditions than under severe-hypoxic conditions. No significant difference was observed between normoxic and hypoxic conditions. pDPCs cultured in low glucose media were significantly more viable than cells cultured in high glucose or glucose (-) media. Error bars represent the mean ± standard deviation for six separate experiments. Statistical analysis was performed using one-way ANOVA and Tukey-Kramer multiple comparison test (From Agata *et al.*, 2008 with modification).

Figure 3

Expression of pluripotent stem cell markers in induced and non-induced pDPCs cultured under severe-hypoxic conditions.

RNA from induced and non-induced pDPCs cultured under severe-hypoxic conditions was extracted at 0, 6, 12, 18, 24 hours. Upregulation of the pluripotent stem cell markers Oct-4 and Sox-2 was observed only in non-induced pDPCs. Oct-4 was transiently activated at 6 hours, followed by the activation of Sox-2 from 12 to 18 hours. Nanog

expression was not observed under any conditions. (From Agata *et al.*, 2008 with modification)

Figure 4

Differentiation potential of odontogenic cells after ischemic de-differentiation.

Induced and non-induced pDPCs were cultured in serum-free D-MEM at various glucose concentrations and exposed to severe-hypoxia for 24 hours. Surviving cells were then "re"-differentiated. Controls consisted of non-induced and induced pDPCs cultured in serum containing D-MEM with high glucose under normoxia. ALP activity in non-induced pDPCs was significantly higher in all groups under both re-induction (-) and re-induction (+) conditions (5A and 5B). The most significant differences were observed in the low glucose groups. **S** = Severe-hypoxia. Error bars represent the mean ± standard deviation for three separate experiments. Statistical analysis was performed using one-way ANOVA and Tukey-Kramer multiple comparison test (From Agata *et al.*, 2008 with modification).

Figure 1

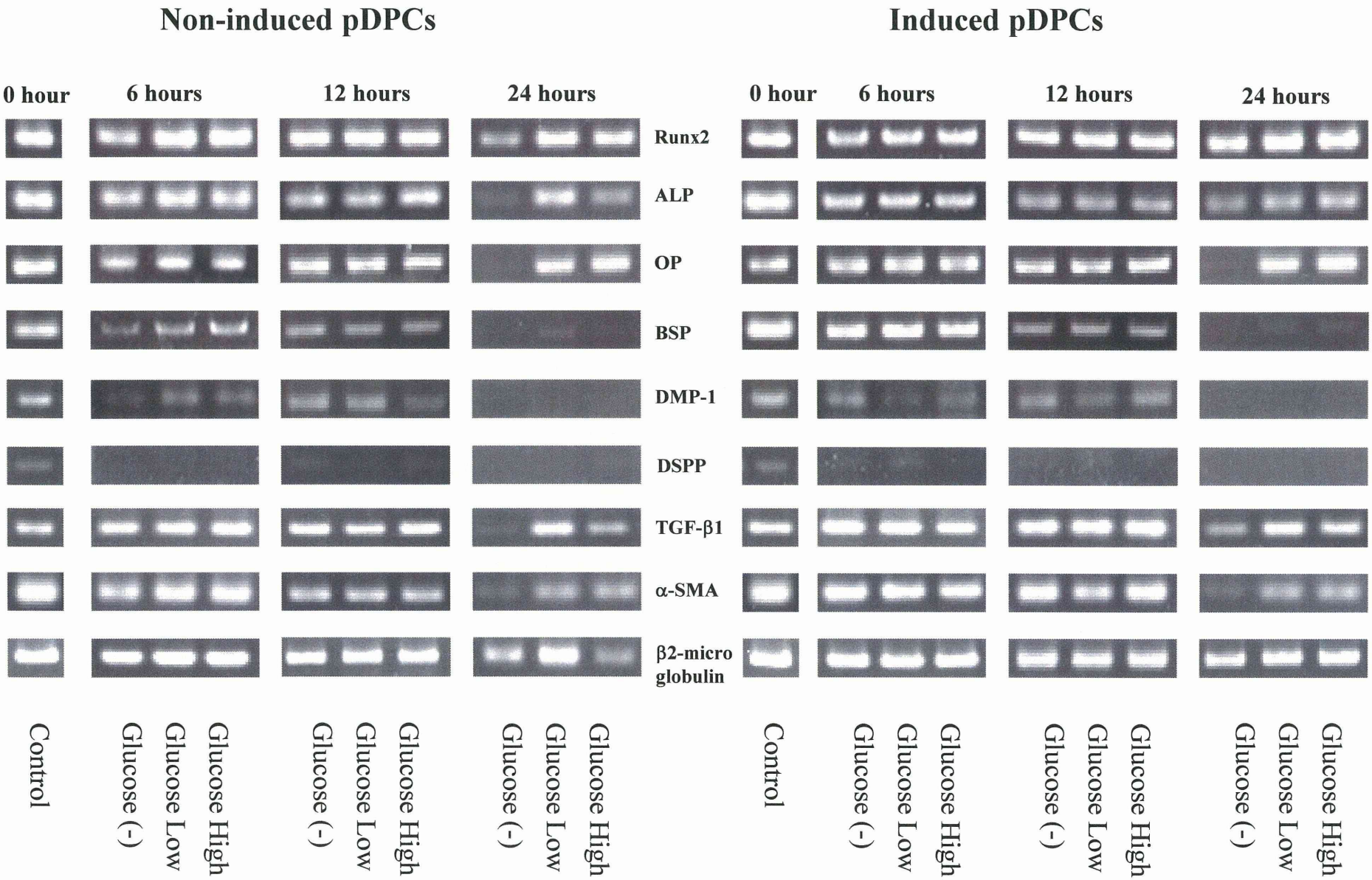
Non-induced pDPCs
Induced pDPCs
0 hour
6 hours
12 hours
24 hours
Runx2
ALP
OP
BSP
DMP-1
DSPP
TGF-β1
α-SMA
β2-micro globulin
Control
Glucose (-)
Glucose Low
Glucose High

Figure 2

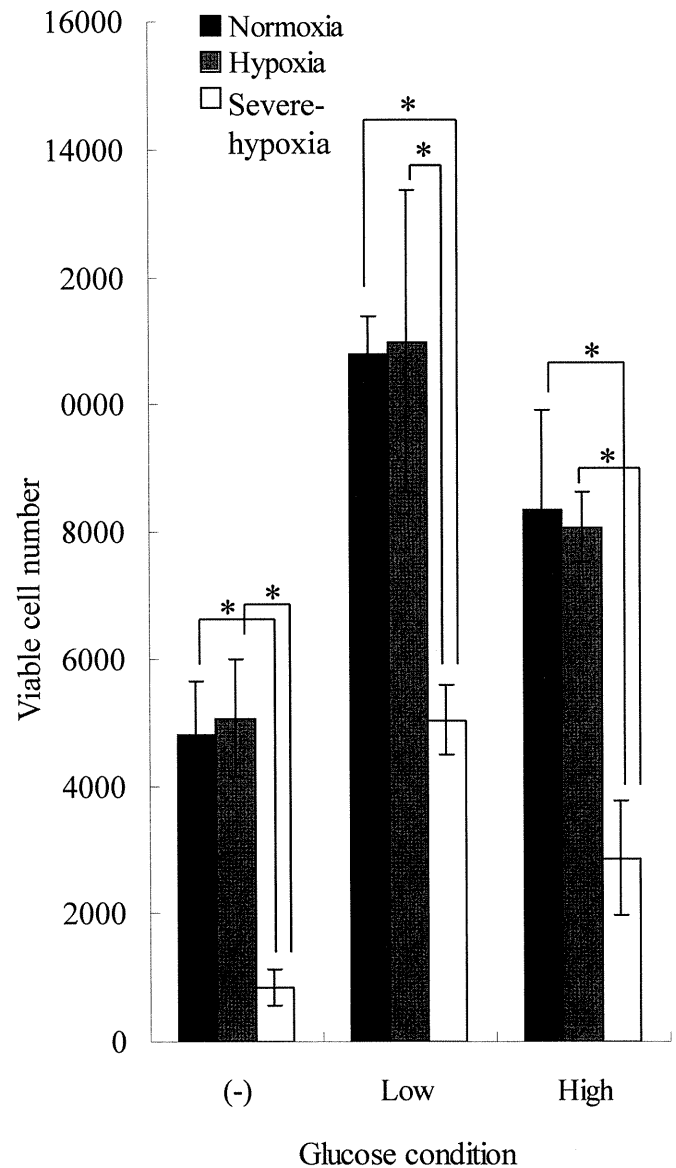
16000
14000
2000
0000
8000
6000
4000
2000
0
Viable cell number
Normoxia
Hypoxia
Severe-
hypoxia
*
*
*
*
*
*
(-)
Low
High
Glucose condition

Figure 3

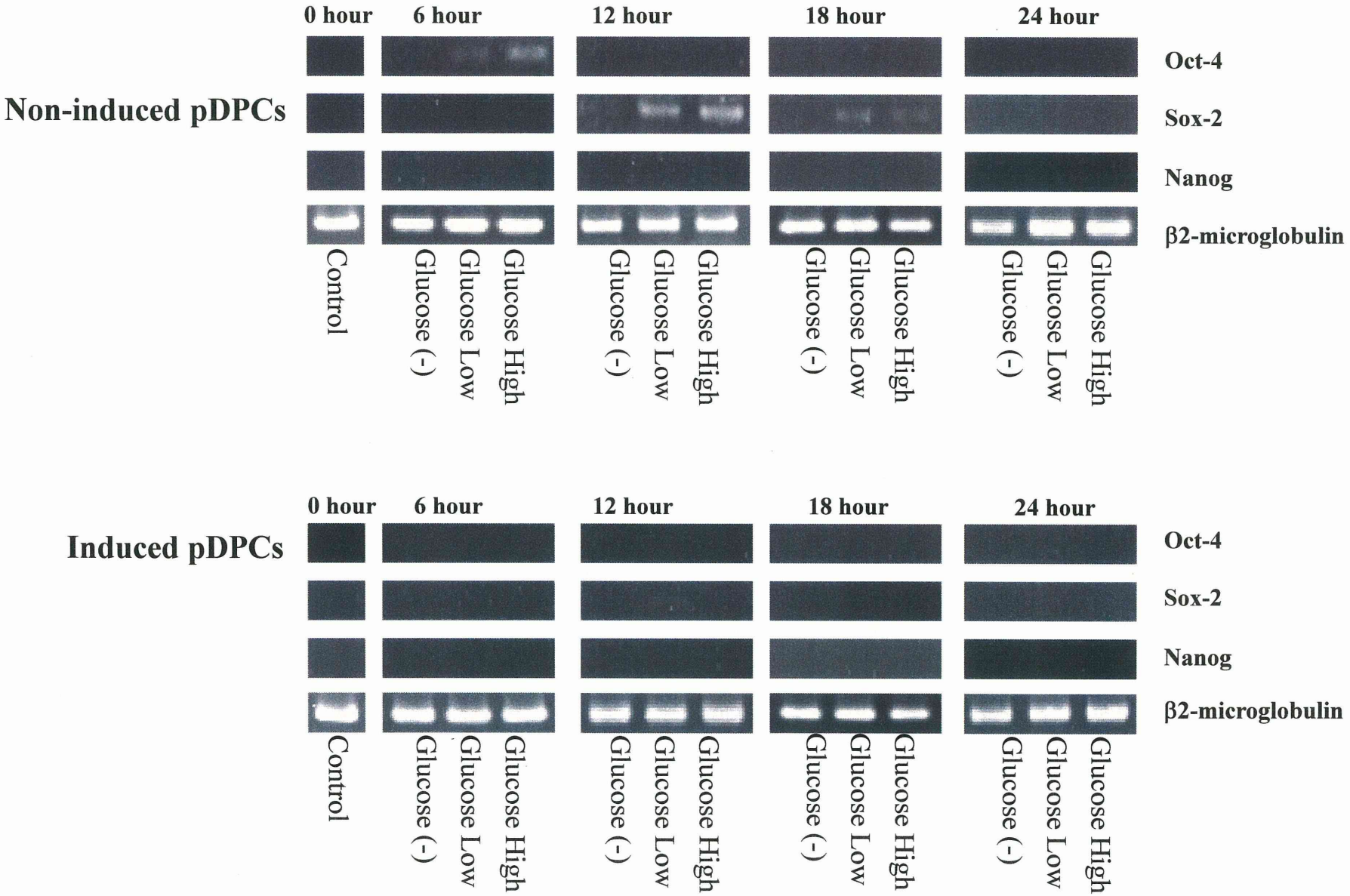
Non-induced pDPCs
0 hour
6 hour
12 hour
18 hour
24 hour
Oct-4
Sox-2
Nanog
β2-microglobulin
Control
Glucose (-)
Glucose Low
Glucose High
Induced pDPCs
0 hour
6 hour
12 hour
18 hour
24 hour
Oct-4
Sox-2
Nanog
β2-microglobulin
Control
Glucose (-)
Glucose Low
Glucose High

Figure 4

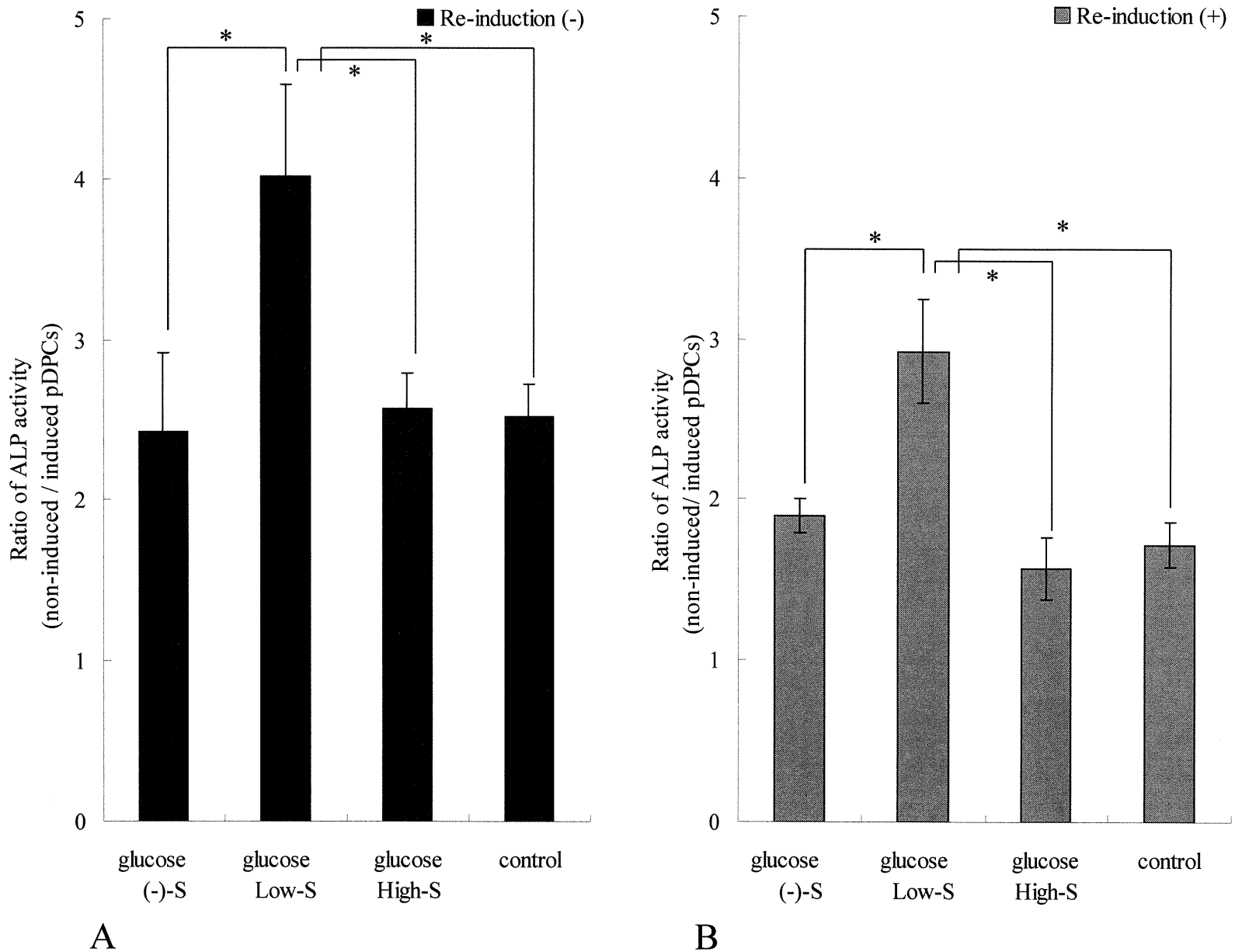
Re-induction (-)
Ratio of ALP activity
(non-induced / induced pDPCs)
5
4
3
2
1
0
*
*
*
glucose
(-)-S
glucose
Low-S
glucose
High-S
control
A
Re-induction (+)
Ratio of ALP activity
(non-induced/ induced pDPCs)
5
4
3
2
1
0
*
*
*
glucose
(-)-S
glucose
Low-S
glucose
High-S
control
B

OPEN ACCESS Freely available online

PLOS ONE

The CD3 versus CD7 Plot in Multicolor Flow Cytometry Reflects Progression of Disease Stage in Patients Infected with HTLV-I

Seiichiro Kobayashi[1], Yamin Tian[1,2], Nobuhiro Ohno[3], Koichiro Yuji[3], Tomohiro Ishigaki[4], Masamichi Isobe[3], Mayuko Tsuda[3], Naoki Oyaizu[5], Eri Watanabe[4], Nobukazu Watanabe[4], Kenzaburo Tani[2], Arinobu Tojo[1,3], Kaoru Uchimaru[3]*

1 Division of Molecular Therapy, Institute of Medical Science, The University of Tokyo, Tokyo, Japan, **2** Department of Molecular Genetics, Medical Institute of Bioregulation, Kyushu University, Fukuoka, Japan, **3** Department of Hematology/Oncology, Research Hospital, Institute of Medical Science, The University of Tokyo, Tokyo, Japan, **4** Laboratory of Diagnostic Medicine, Division of Stem Cell Therapy, Institute of Medical Science, The University of Tokyo, Tokyo, Japan, **5** Clinical Laboratory, Research Hospital, Institute of Medical Science, The University of Tokyo, Tokyo, Japan

Abstract

Purpose: In a recent study to purify adult T-cell leukemia-lymphoma (ATL) cells from acute-type patients by flow cytometry, three subpopulations were observed in a CD3 versus CD7 plot (H: $CD3^{high}CD7^{high}$; D: $CD3^{dim}CD7^{dim}$; L: $CD3^{dim}CD7^{low}$). The majority of leukemia cells were enriched in the L subpopulation and the same clone was included in the D and L subpopulations, suggesting clonal evolution. In this study, we analyzed patients with indolent-type ATL and human T-cell leukemia virus type I (HTLV-I) asymptomatic carriers (ACs) to see whether the CD3 versus CD7 profile reflected progression in the properties of HTLV-I-infected cells.

Experimental Design: Using peripheral blood mononuclear cells from patient samples, we performed multi-color flow cytometry. Cells that underwent fluorescence-activated cell sorting were subjected to molecular analyses, including inverse long PCR.

Results: In the D(%) versus L(%) plot, patient data could largely be categorized into three groups (Group 1: AC; Group 2: smoldering- and chronic-type ATL; and Group 3: acute-type ATL). Some exceptions, however, were noted (*e.g.*, ACs in Group 2). In the follow-up of some patients, clinical disease progression correlated well with the CD3 versus CD7 profile. In clonality analysis, we clearly detected a major clone in the D and L subpopulations in ATL cases and, intriguingly, in some ACs in Group 2.

Conclusion: We propose that the CD3 versus CD7 plot reflects progression of disease stage in patients infected with HTLV-I. The CD3 versus CD7 profile will be a new indicator, along with high proviral load, for HTLV-I ACs in forecasting disease progression.

Citation: Kobayashi S, Tian Y, Ohno N, Yuji K, Ishigaki T, et al. (2013) The CD3 versus CD7 Plot in Multicolor Flow Cytometry Reflects Progression of Disease Stage in Patients Infected with HTLV-I. PLoS ONE 8(1): e53728. doi:10.1371/journal.pone.0053728

Editor: Jean-Pierre Vartanian, Institut Pasteur, France

Received August 31, 2012; **Accepted** December 4, 2012; **Published** January 22, 2013

Funding: This study was supported by the Ministry of Education, Culture, Sports, Science and Technology, Japan. The funders had no role in study design, data collection and analysis, decision to publish, or preparation of the manuscript.

Competing Interests: The authors have declared that no competing interests exist.

* E-mail: uchimaru@ims.u-tokyo.ac.jp

Introduction

Human T-cell leukemia virus type I (HTLV-I) is the agent that causes HTLV-I-associated diseases, such as adult T-cell leukemia-lymphoma (ATL), HTLV-I-associated myelopathy/tropical spastic paraparesis (HAM/TSP), and HTLV-I uveitis (HU) [1–3]. Approximately 10–20 million people are infected with the HTLV-I virus worldwide [4]. The lifetime risk of developing ATL is estimated to be approximately 2.5–5% [5,6]. ATL includes a spectrum of diseases that are referred to as smoldering-, chronic-, lymphoma-, and acute-type [7,8]. The chronic and smoldering types of ATL are considered indolent and are usually managed with watchful waiting until the disease progresses to aggressive (lymphoma- or acute-type) ATL [9]. Because the prognosis of ATL is poor with current treatment strategies, factors to forecast progression to ATL from asymptomatic carriers (ACs) have been researched [10–13] in the hope that they will be useful for preventive therapy under development in the early malignant stage.

Various cellular dysfunctions induced by viral genes (*e.g.*, tax and HBZ), genetic and epigenetic alterations, and the host immune system are considered to cooperatively contribute to leukemogenesis in ATL [14–16]. However, the complex mechanism may hinder determination of a clear mechanism of the pathology and make discovery of risk factors difficult. In a prospective nationwide study in Japan, high proviral load (VL,

Table 1. Clinical profile of patients infected with HTLV-I and normal controls.

Clinical sutype	Number of cases	Male	Female	Age (range)	WBC(/μl) (range)	Lymphocytes(%) (range)	Abnormal lymphocytes(%) (range)
HTLV-1 AC	40	12	28	49.9 (28–70)	5525 (2680–10360)	35.9 (22.4–59.5)	0.9 (0.0–4.4)
Smoldering	7	4	3	55.3 (43–77)	5944 (3680–8710)	32.5 (13.4–47.5)	5.8 (0.7–16.5)
Chronic	7	4	3	52.7 (37–60)	9180 (4070–12790)	45.8 (35.0–61.5)	9.2 (3.4–12.7)
Acute	13	4	9	58.8 (42–74)	15328 (4450–41480)	16.3 (1.7–50.5)	40.3 (3.0–89.6)
Normal controls	10	6	4	47.4 (27–66)	ND	ND	ND

WBC: white blood cells (normal range, 3500–9100/μl).
AC: asymptomatic carrier.
ND: analysis were not performed.
Average of age, WBC, lymphocytes (%) and abnormal lymphocytes (%) are shown.
The proportion of abonormal lymphocytes in peripheral blood WBCs was evaluated by morphological exmanination.
doi:10.1371/journal.pone.0053728.t001

over 4.17 copies/100 peripheral blood mononuclear cells) was found to be a major risk factor for HTLV-I AC developing into ATL [13]. Although VL indicates the proportion of HTLV-I-infected cells, it does not indicate size or degree of malignant progression in each clone; *i.e.*, it does not directly indicate progression of disease stage in HTLV-I infection. Moreover, the majority of ACs with high VL remained intact during the study period, indicating that a more accurate indicator of progression is needed.

In our recent study to purify monoclonal ATL cells from acute-type patients by flow cytometry, three subpopulations were observed in a CD3 versus CD7 plot of $CD4^+$ cells (H: $CD3^{high}CD7^{high}$, D: $CD3^{dim}CD7^{dim}$, L: $CD3^{dim}CD7^{low}$), and the majority of ATL cells were enriched in the L subpopulation [17]. Clonality analyses revealed that the D and L subpopulations contained the same clone, suggesting clonal evolution of HTLV-I-infected cells to ATL cells. From these findings, we speculated that the CD3 versus CD7 profile may reflect disease progression in HTLV-I infection. In this study, the CD3 versus CD7 profile by flow cytometry, combined with molecular (clonality and proviral load) characterizations, were analyzed in patients with various clinical subtypes (HTLV-I AC, and indolent and aggressive ATL). We found that the CD3 versus CD7 profile reflected disease progression of HTLV-I-infected cells to ATL cells. We also discuss the significance of this analysis as a novel risk indicator for HTLV-I ACs in forecasting progression to ATL.

Materials and Methods

Cell lines and patient samples

TL-Om1, an HTLV-I-infected cell line, established Dr. Hinuma's laboratory [18], was provided by Dr. Toshiki Watanabe (The University of Tokyo, Tokyo, Japan) and was cultured in RPMI-1640 medium containing 10% fetal bovine serum. Peripheral blood samples were collected from inpatients and outpatients at our hospital from August 2009 to November 2011. All patients with ATL were categorized according to Shimoyama's criteria [7,8]. Patients with various complications, such as autoimmune disorder and systemic infections, were excluded. Lymphoma-type patients were excluded because ATL cells are not considered to exist in peripheral blood of this clinical subtype. In patients with ATL receiving chemotherapy, blood samples were collected before treatment or during the recovery phase between chemotherapy sessions. Samples collected from 10 healthy volunteers (mean age: 47.4 years; range: 27–66 years) were used as normal controls.

The present study was approved by the research ethics committee of the institute of medical science, the university of Tokyo. Subjects provided written informed consent.

Flow cytometry and cell sorting

Peripheral blood mononuclear cells (PBMCs) were isolated from heparin-treated whole blood by density gradient centrifugation, as described previously [17]. Cells were stained using a combination of phycoerythrin (PE)-CD7, APC-Cy7-CD3, Pacific Blue-CD4, and Pacific Orange-CD14. Pacific Orange-CD14 was purchased from Caltag-Invitrogen (Carlsbad, CA). All other antibodies were obtained from BD BioSciences (San Jose, CA). Propidium iodide (PI; Sigma, St. Louis, MO) was added to the samples to stain dead cells immediately prior to flow cytometry. A BD FACS Aria instrument (BD Immunocytometry Systems, San Jose, CA) was used for all multicolor flow cytometry and cell sorting. Data were analyzed using the FlowJo software (Treestar, San Carlos, CA).

Quantification of HTLV-I proviral load by real-time quantitative polymerase chain reaction (PCR)

The HTLV-I proviral load in FACS-sorted PBMCs was quantified by real-time quantitative polymerase chain reaction (PCR; TaqMan method) using the ABI Prism 7000 sequence detection system (Applied Biosystems, Foster City, CA) as described previously [13,17]. Briefly, 50 ng of genomic DNA was extracted from human PBMCs using a QIAamp DNA blood Micro kit (Qiagen, Hilden, Germany). Triplicate samples of the DNA were amplified. Each PCR mixture, containing an HTLV-I pX region-specific primer pair at 0.1 μM (forward primer 5′-CGGATACCCAGTCTACGTGTT-3′ and reverse primer 5′-

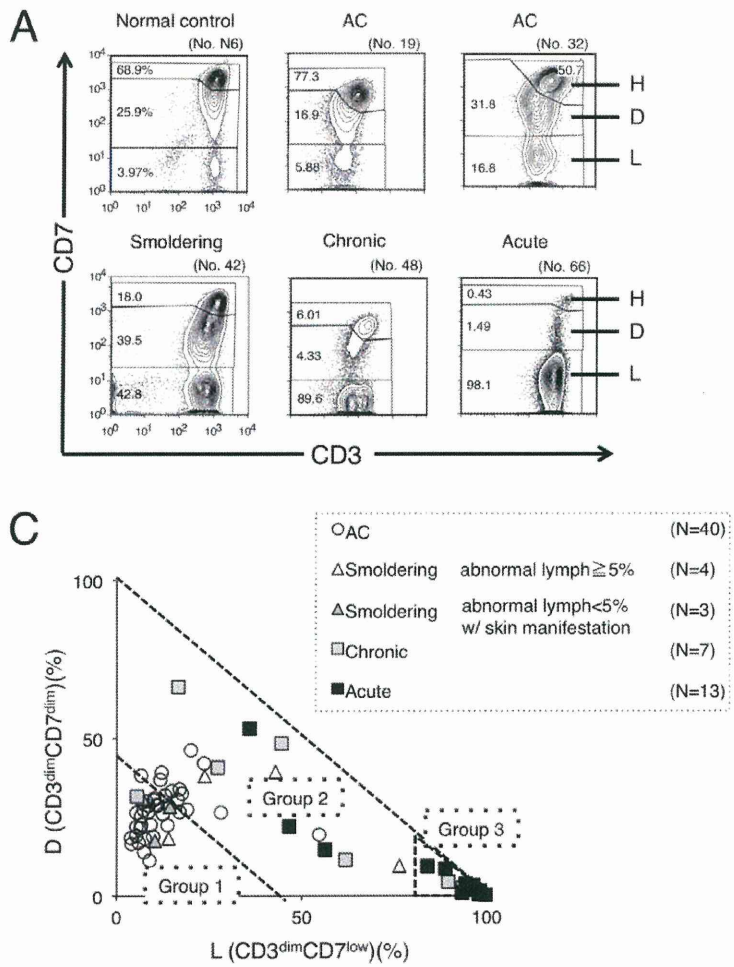

Figure 1. CD3 versus CD7 plots in flow cytometric analysis of patients who are asymptomatic HTLV-I carriers (ACs) and have various clinical subtypes of adult T-cell leukemia-lymphoma (ATL) suggest disease progression in HTLV-I infection. (A) Flow cytometric profile of an AC, various clinical subtypes of ATL (smoldering, chronic, and acute), and a normal control. Representative cases of CD3 versus CD7 plots in $CD4^+$ cells are shown. (B) A two-dimensional plot of AC cases showing the percentage of the D and L subpopulations by flow cytometry. AC cases were divided into two groups according to HTLV-I VL (greater or less than 4%). The border line (45% of D+L subpopulations) between Group 1 and 2 was set based on proviral load (VL). All AC cases with less than 4% VL were included in Group 1. All AC cases included in Group 2 had greater than 4% VL. VL<4%: n = 21; VL>4%: n = 19. All VL data in this figure were provided from the database of the Joint Study on Predisposing Factors of ATL Development (JSPFAD). (C) A two-dimensional plot of all patients showing the percentage of the D and L subpopulations. The smoldering type was divided into two categories: smoldering type with greater than 5% abnormal lymphocytes and smoldering type with less than 5% abnormal lymphocytes with skin manifestation. The two diagonal dotted lines indicate 45% and 100% of D+L subpopulations (*i.e.*, 55% and 0% of the H subpopulation). Data were categorized into three groups.
doi:10.1371/journal.pone.0053728.g001

CAGTAGGGCGTGACGATGTA-3′), FAM-labeled probe at 0.1 μM (5′- CTGTGTACAAGGCGACTGGTGCC-3′), and 1× TaqMan Universal PCR master mix (Applied Biosystems), was subjected to 50 cycles of denaturation (95°C, 15 seconds) and annealing to extension (60°C, 1 minute), following an initial Taq polymerase activation step (95°C, 10 minutes). The RNase P control reagent (Applied Biosystems) was used as an internal control for calculating the input cell number (using VIC reporter dye). DNAs extracted from TL-Om1 and normal human PBMCs were used as positive and negative controls, respectively. The HTLV-I proviral load (%) was calculated as the copy number of the pX region per input cell number. To correct the deviation of data acquired in each experiment, data from TL-Om1 (positive control) were adjusted to 100%, and the sample data were corrected accordingly by a proportional calculation.

Inverse long PCR

For clonality analysis, inverse long PCR was performed [17]. First, 1 μg of genomic DNA extracted from the FACS-sorted cells was digested with *Eco*RI and *Pst*I at 37°C overnight. Purification of DNA fragments was performed using a QIAEX2 gel extraction kit (Qiagen). The purified DNA was self-ligated with T4 DNA ligase (Takara Bio, Otsu, Japan) at 16°C overnight. The circular DNA obtained from the *Eco*RI digestion fragment was then digested

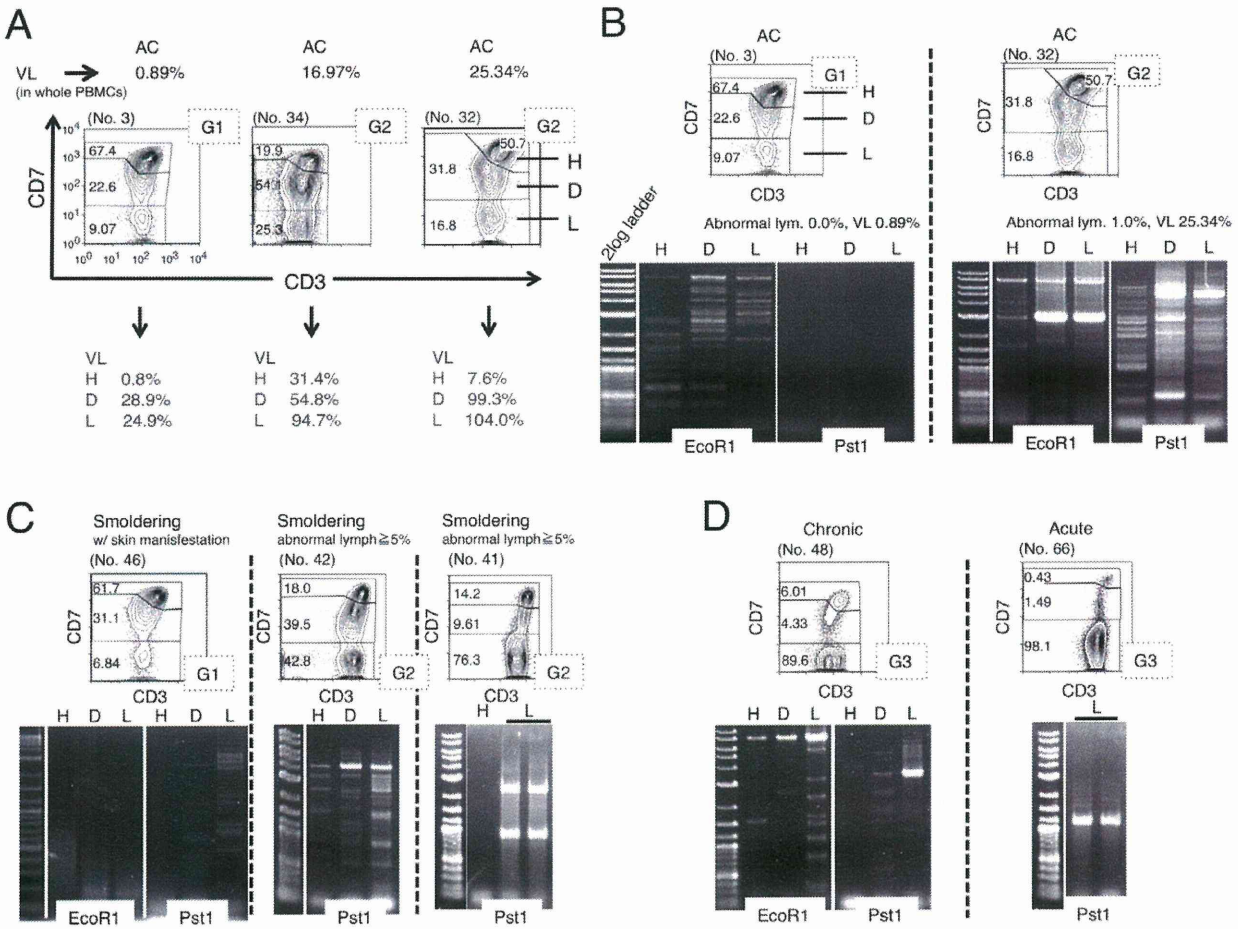

Figure 2. HTLV-I proviral load (VL) and clonality in each subpopulation, based on the CD3 versus CD7 plot. (A) The three subpopulations (H, D, L) based on the CD3 versus CD7 plot were subjected to fluorescence-activated cell sorting (FACS) and VL analysis. Three representative cases are shown. G1 or G2 in the dotted box indicates Group 1 or Group 2, categorized by the percentage of the D and L subpopulations, respectively. (B)–(D) Analysis of clonality in the three subpopulations based on the CD3 versus CD7 plot. Genomic DNA was extracted from FACS-sorted cells of each subpopulation and subjected to inverse long polymerase chain reaction (PCR). Representative data of two cases of AC (B), three cases of smoldering type, including one with skin manifestations (C), and cases of a chronic type and an acute type (D) are shown. PCR was performed in duplicate (black bars) in cases when a sufficient amount of DNA was obtained.
doi:10.1371/journal.pone.0053728.g002

with *Mlu*I, which cuts the pX region of the HTLV-I genome and prevents amplification of the viral genome. Inverse long PCR was performed using Takara LA *Taq* polymerase (Takara Bio). For the *Eco*RI-treated template, the forward primer was 5′-TGCCTGACCCTGCTTGCTCAACTCTACGTCTTTG-3′ and the reverse primer was 5′-AGTCTGGGCCCT-GACCTTTTCAGACTTCTGTTTC-3′. For the *Pst*I-treated group, the forward primer was 5′-CAGCCCATTCTATAG-CACTCTCCAGGAGAG-3′ and the reverse primer was 5′-CAGTCTCCAAACACGTAGACTGGGTATCCG-3. Each 50-μL reaction mixture contained 0.4 mM of each dNTP, 25 mM $MgCl_2$, 10× LA PCR buffer II containing 20 mM Tris-HCl and 100 mM KCl, 0.5 mM of each primer, 2.5 U LA *Taq* polymerase, and 50 ng of the processed genomic DNA. The reaction mixture was subjected to 35 cycles of denaturation (94°C, 30 seconds) and annealing to extension (68°C, 8 minutes). Following PCR, the products were subjected to electrophoresis on 0.8% agarose gels. In samples from which a sufficient amount of DNA was extracted, PCRs were performed in duplicate.

Results

CD3 versus CD7 profile in flow cytometry in various clinical subtypes of patients infected with HTLV-I

The clinical profiles of the 77 cases analyzed in this study are shown in Table 1. According to the gating procedure, as shown in Figure S1 [17], we constructed a CD3 versus CD7 plot of $CD4^+$ cells in PBMCs of various clinical subtypes from patients infected with HTLV-I and normal controls. The three subpopulations ($CD3^{high}CD7^{high}$, $CD3^{dim}CD7^{dim}$, and $CD3^{dim}CD7^{low}$) observed are referred to as the H, D, and L subpopulations, respectively. Representative results for each clinical subtype of HTLV-I infection are shown in Figure 1A. Regarding the data for an acute-type patient (no. 66), the dominant population was the L subpopulation, in which we previously demonstrated that monoclonal ATL cells are enriched [17]. Regarding the AC (no. 19), the CD3 versus CD7 profile was close to that of the normal control, although in some AC cases, such as no. 32, the profile differed from that of the normal control, because in contrast to case no. 19,

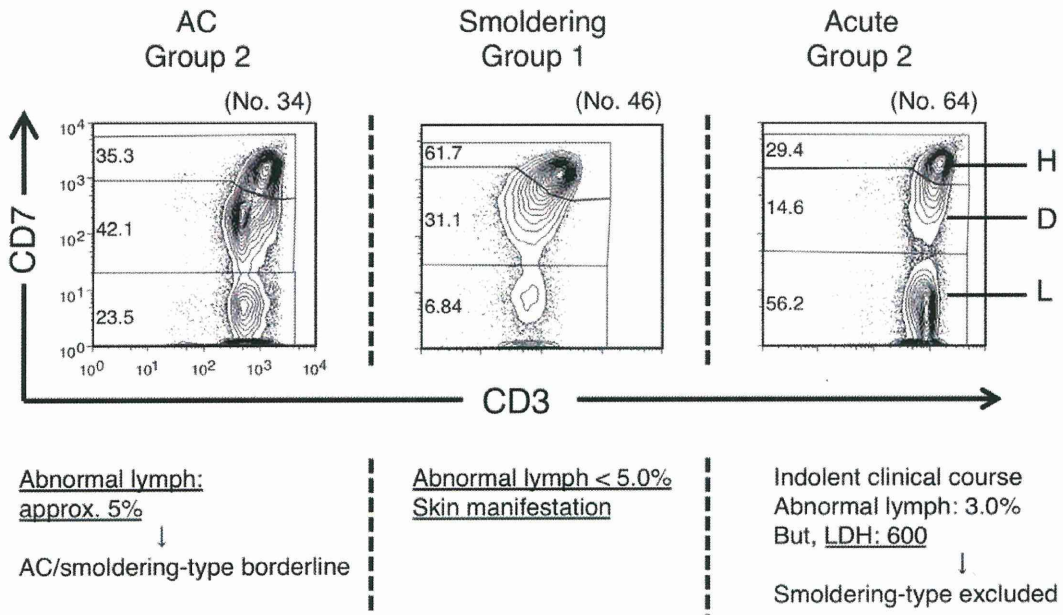

Figure 3. Study of exceptional cases categorized by proportion of the $CD3^{dim}CD7^{dim}$ (D) and $CD3^{dim}CD7^{low}$ (L) subpopulations. Left: An HTLV-I AC patient who was categorized in Group 2 in the D(%) versus L(%) plot. Middle: A patient with smoldering-type ATL who was categorized in Group 1. Right: A patient with acute-type ATL who was categorized in Group 2.
doi:10.1371/journal.pone.0053728.g003

these cases had increased D and L subpopulations. Regarding the data for indolent-type disease (smoldering and chronic), increases in the D and L subpopulations were intermediate between ACs and patients with acute-type disease. These representative flow cytometric data suggest that continuity in the CD3 versus CD7 profile seemed to exist among the various clinical subtypes of patients infected with HTLV-I.

The proportions of D and L subpopulations in all AC cases analyzed are shown in Figure 1B. Because the high HTLV-I proviral load (VL) in whole PBMCs, a VL of >4%, was reported to be a major risk indicator for progression to ATL [13], a border line was set based on VL. Group 1, the area under the diagonal line (D+L = 45%), included all AC cases with VLs of <4%. ACs with VLs of >4% were distributed between Groups 1 and 2. The proportions of D and L subpopulations in normal controls are shown in Figure S2. In this plot, all data for normal controls were distributed in Group 1. Data for all clinical subtypes are shown in Figure 1C. Most data for acute-type patients were located in the area beyond 80% of the L subpopulation and we designated this area as Group 3. Group 2, which is located between Group 1 and Group 3, included the majority of indolent-type (smoldering and chronic) cases. From these results, the three groups in the D(%) versus L(%) plot seemed to represent disease stage in each case.

Proviral load and clonality in each subpopulation in the CD3 versus CD7 plot

To further characterize each subpopulation (H, D, and L) in the CD3 versus CD7 plot, cells in each subpopulation were FACS-sorted and subjected to analysis of VL to determine the percentage of HTLV-I-infected cells in each subpopulation. Results for representative cases are shown in Figure 2A. The VL in whole PBMCs of an AC (no. 3) was low (0.89%). As expected, the VL in H, the major subpopulation, was low (0.8%). However, VLs in the D and L subpopulations were considerably higher (28.9% and 24.9%, respectively), indicating that HTLV-I-infected cells are relatively concentrated in these subpopulations. In the cases with high VLs in whole PBMCs (no. 32 with 25.34%; no. 34 with 16.97%), the VLs were also higher in the D and L subpopulations, and almost all cells in the L subpopulation were HTLV-I-infected.

In HTLV-I infection, progression to ATL requires several pathological steps, including clonal expansion [15]. To further characterize the three subpopulations based on the CD3 versus CD7 plot, we analyzed clonality in each subpopulation in patients with various clinical subtypes using the inverse long PCR method. Figure 2B shows two cases of AC. In the left case (no. 3), included in Group 1 in the D(%) and L(%) plot, multiple bands suggestive of multiple small clones were detected in the three subpopulations. However, no major band suggestive of a dominant clone was observed. In the right case (no. 32), included in Group 2, inverse long PCR of the FACS-sorted subpopulations suggested that the D and L subpopulations contained a major clone (Figure 2B). The D subpopulation had bands of the same size as those of the L subpopulation, indicating that the two distinct subpopulations contained a common major clone. Eleven cases of AC were included in Group 2. All three cases analyzed by Southern blotting (whole blood samples) were positive for clonal bands (Figure S3). In Figure 2C, data for three smoldering cases are shown. In case no. 46 (left), whose only manifestation was a skin eruption with few abnormal lymphocytes (less than 5% of white blood cells) in the peripheral blood, only faint minor bands suggestive of small clones were observed. In contrast, in the other two cases (nos. 42 and 41), intense bands suggestive of major clones were observed in both the D and L subpopulations. In no. 41 (right), weak bands were not visible, which suggested the selection of dominant clones. In Figure 2D, data for a chronic-type case and an acute-type case are shown. In both cases, intense bands in the L subpopulation suggest the existence of a major clone. The series of clonality analyses indicated that a major clone became more evident and the clinical

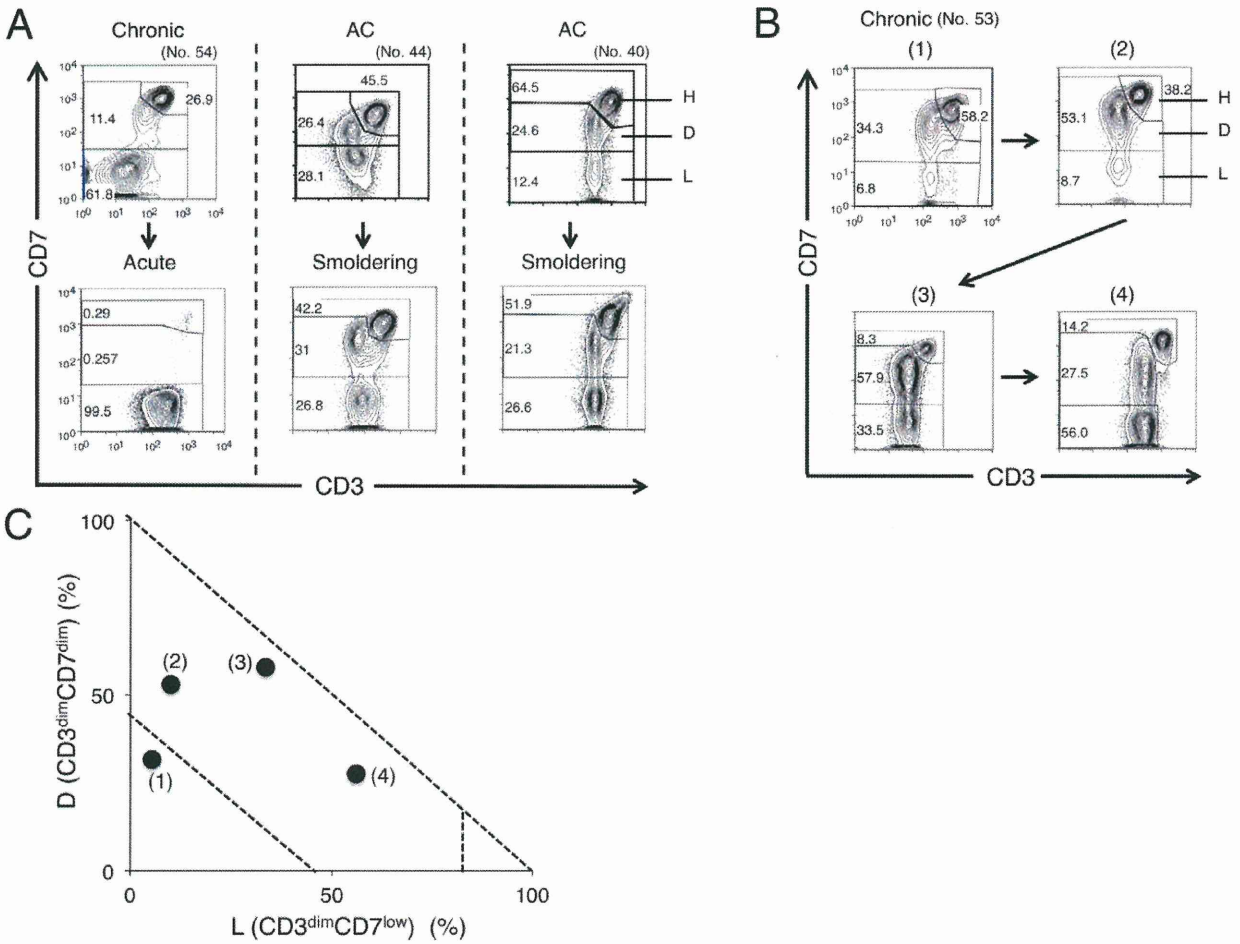

Figure 4. Alteration in the CD3 versus CD7 profile by flow cytometry in accordance with disease progression. (A) Change in the CD3 versus CD7 profile in representative cases. In all three cases shown, change in clinical data (*e.g.*, abnormal lymphocyte, LDH) resulted in progression of the clinical subtype. (B) Change in the CD3 versus CD7 profile in a time course in the case of chronic-type ATL. Clinical data are shown in Table S1. (C) Flow cytometric data in (B) are summarized in the D(%) versus L(%) plot.
doi:10.1371/journal.pone.0053728.g004

stage became more advanced as the D and L subpopulations increased.

Clinical evaluation of exceptional cases categorized by proportions of the $CD3^{dim}CD7^{dim}$ (D) and $CD3^{dim}CD7^{low}$ (L) subpopulations

As noted above, the D(%) versus L(%) plot generally represented disease stage in HTLV-I infection. However, we observed one case of chronic-type disease and three cases of smoldering-type disease in Group 1 and three cases of acute-type disease in Group 2. Furthermore, some ACs with VLs of >4% were observed in Group 2. Representative data from these apparently exceptional cases are shown in Figure 3. On the left, a case of AC (no. 34) observed in Group 2 is shown. 4.7% of lymphocytes in this blood sample were abnormal and clonality analysis by Southern blotting showed oligoclonal bands suggestive of clones of substantial size (Figure S3). These clinical data suggest that the disease stage would be around the AC/smoldering borderline. In the middle, a case of a smoldering type (no. 46) observed in Group 1 is shown. In this case, the percentage of abnormal lymphocytes in the peripheral blood was only 1%, but she had a histologically proven ATL lesion in the skin and was diagnosed with smoldering-type ATL. The other two smoldering cases categorized in Group 1 were the same as this case. These results indicate that ATL cells in these three smoldering cases infiltrated the skin, but not the peripheral blood. On the right, a case of acute-type disease categorized as Group 2 (no. 64) is shown. The clinical course of this patient was relatively indolent compared with typical acute-type disease. He had skin infiltration of ATL cells, but no lymph node swelling. However, LDH exceeded 1.5 times the upper limit of the normal range, which excludes a diagnosis of smoldering-type disease. Other acute-type cases categorized in Group 2 were diagnosed as such according to Shimoyama's criteria, but also had the same indolent clinical course as case no. 64. These cases should have been regarded as indolent ATL.

Changes in the CD3 versus CD7 profile in flow cytometry with disease progression

In several cases, we could obtain time-sequential samples (Figure 4). The patient (no. 54) shown on the left in Figure 4A progressed from chronic-type to acute-type disease. In flow cytometric analysis, decreases in the H and D subpopulations

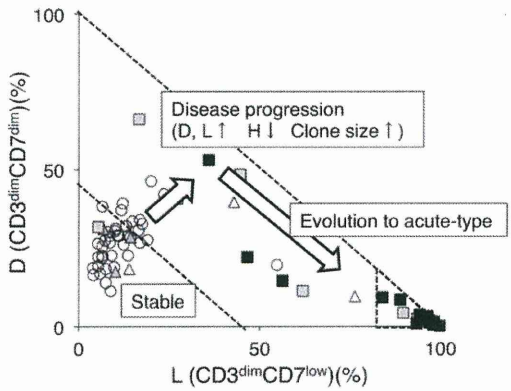

Figure 5. Summary of the study: the CD3 versus CD7 profile reflects progression of disease stage in patients infected with HTLV-I. In the percentage of D ($CD3^{dim}CD7^{dim}$) versus L ($CD3^{dim}CD7^{low}$) plot, Group 1 includes the majority of AC cases. As disease stage progresses, the CD3 versus CD7 profile then changes. With downregulation of CD3 and CD7, the D and L subpopulations increase gradually (Group 2). During this step, clones in the D and L subpopulations increase in size. Further accumulation of genetic alterations will result in rapid expansion of ATL clones—*i.e.*, evolution to acute-type ATL. In this step, the CD3 versus CD7 profile will progress from Group 2 to 3.
doi:10.1371/journal.pone.0053728.g005

and an increase in the L subpopulation were observed, indicating that disease progression correlated well with the change in the CD3 versus CD7 profile. The patients in the middle (no. 44) and on the right (no. 40) were included in Group 2 at the AC stage and later progressed to smoldering-type ATL. Although variation in the change of the flow cytometric profile was seen between these patients, the results suggest that ACs in Group 2 are at high risk of developing ATL.

The patient in Figure 4B (no. 53) was initially diagnosed with AC and later progressed to chronic-type ATL. Although the initial clinical course was stable, an increase in abnormal lymphocyte numbers was later observed, and low-dose VP-16 therapy (50 mg/day) was initiated because of hypoxemia due to lung infiltration of ATL cells. Table S1 and Figure 4C show summaries of the clinical data and the flow cytometric analyses, respectively. The flow cytometric data correlated well with disease progression.

Discussion

Findings in our previous analysis of acute-type ATL samples prompted our analysis of various clinical subtypes of patients infected with HTLV-I to examine whether the CD3 versus CD7 profile reflects the progression of oncogenesis in HTLV-I-infected cells [17]. Representative flow cytometric data shown in Figure 1A suggested that the CD3 versus CD7 profile changed during disease progression. As the disease stage progressed, the D and L subpopulations increased with concomitant decreases in the $CD3^{high}CD7^{high}$(H) subpopulation. Figure 1C, a summary of the flow cytometric data of all cases analyzed, reveals that the two-dimensional plot of the proportions of the D versus L subpopulations could divide all cases into three groups. Group 1, the area under the diagonal line, equivalent to 55% of the H subpopulation in which all normal controls were included (Figure S2), contained the majority of HTLV-I ACs. Group 3 was the area beyond 80% of the L subpopulation, and the majority of acute-type cases were included in this group. Group 2, located between Groups 1 and 3 (*i.e.*, less than 55% of the H subpopulation and 80% of the L subpopulation), included indolent-type (smoldering and chronic) cases and some AC cases. These results suggest that the CD3 versus CD7 expression profile reflects disease stage. Initially, both the D and L subpopulations gradually and simultaneously increased. However, at the clinically advanced stage, the increase in the L subpopulation was prominent. The change is considered to reflect the biological difference between the D and L subpopulations, which needs to be clarified.

In HTLV-I infection, the small clones of infected cells are considered to coexist from the AC stage [19,20]. A selected clone from the multiple small clones then grows and progresses to the malignant state, and the emergence of a dominant clone indicates disease progression in ATL [19,20]. As shown in Figure 2B–D, major bands suggesting dominant clones were evident in patients with progressed clinical subtypes or those in the advanced group in the CD3 versus CD7 profile, and major bands existed exclusively in the D and L subpopulations. These data also support the idea that increases in the D and L subpopulations correlate with the progression of disease stage. AC cases in Group 2 had high HTLV-I proviral loads (>4%; Figure 1B) and clear major bands were observed by inverse long PCR in these cases (Figure 2B, right). Sasaki *et al.* reported that two cases of HTVL-I AC with oligoclonal bands on Southern blots and high VLs (20%) had progressed to ATL by 4 and 3.5 years later [21]. The two cases may correspond to HTLV-I AC in Group 2 proposed in our study. In fact, two cases of ACs in our series that were included in Group 2 progressed to smoldering ATL (Figure 4A). AC cases in Group 2 could be regarded as advanced carriers. Our flow cytometric analysis could apparently discriminate high-risk AC cases from stable ones. Follow-up analysis of these cases is warranted to determine whether AC cases included in Group 2 progress to ATL. Flow cytometric data for these AC cases included in Group 2 (Figure 1A and 1C) were similar to those for indolent ATL cases in Group 2. These ACs in Group 2 can be considered essentially the same as smoldering ATL cases. Some of the ACs categorized according to Shimoyama's criteria should in fact be separated and regarded as a subtype together with at least some of the smoldering ATL cases.

Iwanaga *et al.* reported that high HTLV-I proviral load (>4%) in whole PBMCs was a risk factor for progression to ATL [13]. In Figure 1B, the ACs with VLs>4% were distributed between Groups 1 and 2. These findings suggest that not all ACs with high VLs are currently in an advanced stage, although they may have the potential to develop ATL in the future.

In general, the categorization by flow cytometric profile correlated well with the current classification of clinical subtypes, with some exceptional cases of acute-type and smoldering-type disease (Figure 3). The only manifestation of three smoldering cases categorized in Group 1 was skin lesions; they fell into Group 1 because they showed minimal abnormalities in peripheral blood [22]. Three acute-type ATL cases categorized in Group 2 had indolent clinical courses. A diagnosis of acute-type disease is made when the indolent-type and lymphoma-type are excluded, according to Shimoyama's criteria. The CD3 versus CD7 plot may discriminate the cases that will follow an indolent clinical course from the aggressive acute-type ATL.

The VL in each subpopulation indicated that HTLV-I-infected cells were relatively concentrated in the D and L subpopulations (representative data are shown in Figure 2A). These data are consistent with downregulation of CD3 and CD7 being relevant to HTLV-I infection, although cells without HTLV-I infection may also contribute to this change to some extent, as a substantial subpopulation of T cells has been reported to be CD7-deficient under physiological [23,24] and certain pathological conditions,

including autoimmune disorders and viral infection [25–29]. To more precisely analyze phenotypic changes in HTLV-I-infected cells, markers that indicate HTLV-I infection should be incorporated in future studies.

A summary of this study is shown in Figure 5. In the CD3 versus CD7 profile, most AC cases were included in Group 1, in which the D and L subpopulations were relatively small. Consistent with disease progression to smoldering- and chronic-type ATL, a decrease in the H subpopulation and increases in the D and L subpopulations occur (Group 2). In this step, increases in the sizes of clones in the D and L subpopulations are observed. Further expansion of the leukemic clone results in progression to acute-type ATL in which the L subpopulation has expanded (Group 3). According to a study by Yamaguchi *et al.*, the natural course of ATL is to progress from the HTLV-I carrier state through the intermediate state, smoldering ATL, and chronic ATL, and finally to the acute ATL, indicating a process of multistage leukemogenesis [19]. We consider this study to successfully link the progressive clinical status and phenotypic changes in HTLV-I-infected cells. However, the way in which this profile reflects multistep oncogenesis in HTVL-I infection at the molecular level remains unclear. Further molecular analyses of the three subpopulations will help in understanding the mechanism(s).

Supporting Information

Figure S1 Representative flow cytometric analysis of an HTLV-I asymptomatic carrier (patient no. 32). The CD3 versus CD7 plot of $CD4^+$ cells was constructed according to the gating procedure shown in this figure. In the plot, we designated three subpopulations: H ($CD3^{high}CD7^{high}$), D ($CD3^{dim}CD7^{dim}$), and L ($CD3^{dim}CD7^{low}$).
(PPTX)

Figure S2 A two-dimensional plot of 10 normal controls showing the percentage of the D and L subpopulations.
(PPTX)

Figure S3 Southern blot analysis of clonal integration of the HTLV-I provirus. Representative data (AC, No. 34) are shown. In *Eco*RI or *Pst*I digestion, a band indicated by a red arrow represents the monoclonal integration of the provirus. The band pattern indicates that two major clones coexist. This analysis was performed by a commercial laboratory (SRL, Tokyo, Japan).
(PPTX)

Table S1 Clinical data in a case of chronic-type ATL (No. 53). Proportion of abonormal lymphocytes in the preipheral blood WBC were evaluated by morphological exmanination. LDH: Lactate dehydrogenase (normal range, 120–240 U/L) sIL-2R: soluble interleukin-2 receptor (normal range, 122–496 U/ml).
(XLSX)

Acknowledgments

We thank Dr. Toshiki Watanabe, Dr. Kazumi Nakano, and Dr. Tadanori Yamochi (The University of Tokyo) for providing the TL-Om1 cell line and the plasmid containing the HTLV-I genome, which was used as a standard for the quantification of proviral load. We also thank Mr. Yuji Zaike (Clinical Laboratory, Research Hospital, Institute of Medical Science, The University of Tokyo) for his excellent technical advice. We are grateful to the hospital staff who have made a commitment to providing high-quality care to all of our patients.

Author Contributions

Conceived and designed the experiments: KT AT KU. Performed the experiments: SK YT. Analyzed the data: EW NW TI NO. Contributed reagents/materials/analysis tools: MI MT KU NO. Wrote the paper: SK KU.

References

1. Yoshida M, Miyoshi I, Hinuma Y (1982) Isolation and characterization of retrovirus from cell lines of human adult T-cell leukemia and its implication in the disease. Proc Natl Acad Sci U S A 79: 2031–2035.
2. Osame M, Usuku K, Izumo S, Ijichi N, Amitani H, et al. (1986) HTLV-I associated myelopathy, a new clinical entity. Lancet 1: 1031–1032.
3. Mochizuki M, Watanabe T, Yamaguchi K, Takatsuki K, Yoshimura K, et al. (1992) HTLV-I uveitis: a distinct clinical entity caused by HTLV-I. Japanese journal of cancer research : Gann 83: 236–239.
4. Proietti FA, Carneiro-Proietti AB, Catalan-Soares BC, Murphy EL (2005) Global epidemiology of HTLV-I infection and associated diseases. Oncogene 24: 6058–6068.
5. Yamaguchi K, Watanabe T (2002) Human T lymphotropic virus type-I and adult T-cell leukemia in Japan. International journal of hematology 76 Suppl 2: 240–245.
6. Murphy EL, Hanchard B, Figueroa JP, Gibbs WN, Lofters WS, et al. (1989) Modelling the risk of adult T-cell leukemia/lymphoma in persons infected with human T-lymphotropic virus type I. International journal of cancer Journal international du cancer 43: 250–253.
7. Shimoyama M (1991) Diagnostic criteria and classification of clinical subtypes of adult T-cell leukaemia-lymphoma. A report from the Lymphoma Study Group (1984–87). Br J Haematol 79: 428–437.
8. Tsukasaki K, Hermine O, Bazarbachi A, Ratner L, Ramos JC, et al. (2009) Definition, prognostic factors, treatment, and response criteria of adult T-cell leukemia-lymphoma: a proposal from an international consensus meeting. J Clin Oncol 27: 453–459.
9. Takasaki Y, Iwanaga M, Imaizumi Y, Tawara M, Joh T, et al. (2010) Long-term study of indolent adult T-cell leukemia-lymphoma. Blood 115: 4337–4343.
10. Hisada M, Okayama A, Shioiri S, Spiegelman DL, Stuver SO, et al. (1998) Risk factors for adult T-cell leukemia among carriers of human T-lymphotropic virus type I. Blood 92: 3557–3561.
11. Imaizumi Y, Iwanaga M, Tsukasaki K, Hata T, Tomonaga M, et al. (2005) Natural course of HTLV-1 carriers with monoclonal proliferation of T lymphocytes ("pre-ATL") in a 20-year follow-up study. Blood 105: 903–904.
12. Kamihira S, Atogami S, Sohda H, Momita S, Yamada Y, et al. (1994) Significance of soluble interleukin-2 receptor levels for evaluation of the progression of adult T-cell leukemia. Cancer 73: 2753–2758.
13. Iwanaga M, Watanabe T, Utsunomiya A, Okayama A, Uchimaru K, et al. (2010) Human T-cell leukemia virus type I (HTLV-1) proviral load and disease progression in asymptomatic HTLV-1 carriers: a nationwide prospective study in Japan. Blood 116: 1211–1219.
14. Okamoto T, Ohno Y, Tsugane S, Watanabe S, Shimoyama M, et al. (1989) Multi-step carcinogenesis model for adult T-cell leukemia. Japanese journal of cancer research : Gann 80: 191–195.
15. Matsuoka M, Jeang KT (2007) Human T-cell leukaemia virus type 1 (HTLV-1) infectivity and cellular transformation. Nat Rev Cancer 7: 270–280.
16. Yoshida M (2010) Molecular approach to human leukemia: isolation and characterization of the first human retrovirus HTLV-1 and its impact on tumorigenesis in adult T-cell leukemia. Proceedings of the Japan Academy Series B, Physical and biological sciences 86: 117–130.
17. Tian Y, Kobayashi S, Ohno N, Isobe M, Tsuda M, et al. (2011) Leukemic T cells are specifically enriched in a unique CD3(dim) CD7(low) subpopulation of CD4(+) T cells in acute-type adult T-cell leukemia. Cancer science 102: 569–577.
18. Sugamura K, Fujii M, Kannagi M, Sakitani M, Takeuchi M, et al. (1984) Cell surface phenotypes and expression of viral antigens of various human cell lines carrying human T-cell leukemia virus. International journal of cancer Journal international du cancer 34: 221–228.
19. Yamaguchi K, Kiyokawa T, Nakada K, Yul LS, Asou N, et al. (1988) Polyclonal integration of HTLV-I proviral DNA in lymphocytes from HTLV-I seropositive individuals: an intermediate state between the healthy carrier state and smouldering ATL. British journal of haematology 68: 169–174.
20. Mortreux F, Gabet AS, Wattel E (2003) Molecular and cellular aspects of HTLV-1 associated leukemogenesis in vivo. Leukemia : official journal of the Leukemia Society of America, Leukemia Research Fund, UK 17: 26–38.
21. Sasaki D, Doi Y, Hasegawa H, Yanagihara K, Tsukasaki K, et al. (2010) High human T cell leukemia virus type-1(HTLV-1) provirus load in patients with HTLV-1 carriers complicated with HTLV-1-unrelated disorders. Virology journal 7: 81.
22. Setoyama M, Katahira Y, Kanzaki T (1999) Clinicopathologic analysis of 124 cases of adult T-cell leukemia/lymphoma with cutaneous manifestations: the smouldering type with skin manifestations has a poorer prognosis than previously thought. The Journal of dermatology 26: 785–790.
23. Reinhold U, Abken H (1997) CD4+ CD7- T cells: a separate subpopulation of memory T cells? J Clin Immunol 17: 265–271.